CrystEngComm

RSC Publishing

PAPER

View Article Online
View Journal | View Issue

Cite this: *CrystEngComm*, 2013, **15**, 1244

Construction of homo- and heterometallic-pyridine-2,3-dicarboxylate metallosupramolecular networks with structural diversity: 1D T5(2) water tape and unexpected coordination mode of pyridine-2,3-dicarboxylate†

Fatih Semerci,[ab] Okan Zafer Yeşilel,*[a] Seda Keskin,[c] Cihan Darcan,[d] Murat Taş[e] and Hakan Dal[f]

Received 13th October 2012,
Accepted 17th November 2012

DOI: 10.1039/c2ce26675j

www.rsc.org/crystengcomm

Five new homo and heterometallic Cu(II), Cd(II), Cu(II)–Ag(I), Cu(II)–Cd(II) supramolecular networks with pyridine-2,3-dicarboxylate (pydc), $\{[Cu(\mu\text{-pydc})(dmpen)_2]\}_n$ (**1**), $[Cu_2(\mu\text{-pydc})_2(emim)_4]\cdot 2H_2O$ (**2**), $[Cd(\mu\text{-pydc})(emim)_2]_n$ (**3**), $[Cu(en)_2(H_2O)_2][Ag_2(pydc)_2(\mu\text{-en})]\cdot 6H_2O$ (**4**) and $\{[Cd(H_2O)_4Cu(\mu\text{-pydc})_2]\cdot 2H_2O\}_n$ (**5**) have been synthesized and structurally characterized (en = ethylenediamine, dmpen = 1,3-diamino-2,2-dimethylpropane and emim = 2-ethyl-4-methyl-imidazole). Owing to diverse binding modes and conformations of the pydc ligand and the different diamine or imidazole-containing coligands, these complexes exhibit structural and dimensional diversity. Complex **1** exhibits a new unexpected coordination mode of pydc, which is known as a chelating ligand, leading to the formation of a 1D coordination polymer. Complex **2** is the first dinuclear copper(II)–pydc complex containing a dinuclear metalloligand. Complex **3** is a one dimensional coordination polymer and the Cd(II) ion is six-coordinated in a distorted octahedral geometry. Complex **4** is the first 3d–4d heterometallic complex and shows two different coordination behaviors of the ethylenediamine ligand: common chelate mode and rare bridging mode. The most striking feature of **4** is the existence of a infinite T5(2) water tape. Complex **5** is the first 3d–4d heteropolynuclear complex obtained from a polynuclear metalloligand. Neighboring metalloligand double-chains bind to Cd(II) ions to form a two dimensional (2D) layered structure. Complex **4** exhibits weak emission due to the quenching effect of Cu(II) ions. Complexes **3** and **5** exhibit rare green emission and blue photoluminesence, respectively. Atomically detailed simulations were used to assess the potential of complexes in gas storage and gas separation applications. The antimicrobial properties of the complexes were also investigated by the broth dilution method (MIC). Complexes **4** and **5** are determined to be highly effective for antimicrobial activity.

Introduction

Supramolecular assembly of coordination polymers is an emerging area of research with their intriguing topological structures and several potential applications in areas such as catalysis, conductivity, porosity, chirality, luminescence, magnetism, spin-transition and non-linear optics.[1–8] Weak intermolecular forces have been used in intentional strategies for connecting coordination compounds into a wide variety of extended networks and these results have shown that hydrogen bonds acting in concert are capable of marshalling mononuclear, dinuclear, polynuclear or heteronuclear large complex ions into desirable motifs.[9–15] In the construction of supramolecular networks, water is usually used as a solvent.

[a]*Department of Chemistry, Faculty of Arts Sciences, Eskişehir Osmangazi University, 26480 Eskişehir, Turkey. E-mail: yesilel@ogu.edu.tr; Fax: +90 222 239357; Tel: +90 222 2393750*
[b]*Department of Chemistry, Faculty of Arts and Sciences, Kırklareli University, 39100 Kırklareli, Turkey*
[c]*Department of Chemical and Biological Engineering, Koç University, İstanbul, Turkey*
[d]*Department of Molecular Biology and Genetic, Faculty of Arts and Sciences, Bilecik Şeyh Edebali University, 11000 Bilecik, Turkey*
[e]*Department of Chemistry, Faculty of Arts and Sciences, Giresun University, Giresun, Turkey*
[f]*Department of Chemistry, Faculty of Sciences, Anadolu University, Eskişehir, Turkey*
† Electronic supplementary information (ESI) available. CCDC 887870–887874. For ESI and crystallographic data in CIF or other electronic format see DOI: 10.1039/c2ce26675j

These water clusters which are structurally embedded in coordination polymer through the hydrogen bonds support the assembly together with supramolecular networks.[16–19]

At the beginning of this new century, the introduction of functionality into polymetallic and heterometallic systems has become one of the aims of a good number of research groups working in coordination chemistry.[20–22] The attraction of bimetallic coordination polymers is that the simultaneous presence of two different metals can potentially give rise to more complex physical properties and structural diversity.[23–27] Because of the diversity of the coordination modes and high structural stability, multidentate organic aromatic polycarboxylate ligands have been used to assemble supramolecular networks organized by coordination bonds and non-covalent interactions, especially hydrogen bonds. Pyridinedicarboxylic acids have proved to be interesting versatile ligands and may exhibit various coordination modes to furnish various structures with high dimensions.[28,29] In addition to pyridinedicarboxylic acids, the use of bifunctional pyridine-2,3-dicarboxylic acid ($pydcH_2$) as a bridging ligand to react with transition metals has been known for its diverse coordination abilities as a result of the asymmetric coordination environments of the carboxylate groups at the 2- and 3-positions of the pyridine ring that provide variable bridging and coordination modes.[27–40] Pyridine-2,3-dicarboxylic acid is remarkably attractive for its flexible and various coordination modes to construct mononuclear, dinuclear or polynuclear architecture. The deprotonated pyridinedicarboxylates ($pydc^{2-}$ and $pydcH^{-}$) are useful tools for constructing crystalline architectures because of their proton donating and accepting capabilities for hydrogen bonding and their pyridine ring for aromatic interactions. These ligands are also attractive due to their biological activities including neurotoxic and antimicrobial activities.[41–45]

The combination of metal ions or clusters and organic ligands in coordination polymers provides an efficient route to a new type of photoluminescent material with potential applications.[46–52] Complexes consisting of d^{10} metals have been shown to exhibit interesting photoluminescent properties.[53–56]

The driving force behind the comprehensive experimental and theoretical researches on water clusters lies in understanding the unusual properties of bulk water.[19] Water clusters are widespread in nature and play a significant role in the stabilization of supramolecular systems in the solid state.[17] The structural elucidation of water clusters in supramolecular system is the key to gain insight into the nature of hydrogen bond.[57]

Recent studies showed that coordination polymers exhibit good potential in gas adsorption and gas separation applications due to their well-defined pores, high pore volumes, large surface areas and a large variety of chemical functionalities.[58]

In this study, five new metallosupramolecular networks built by 2,3-pyridinedicarboxylic acid were synthesized and structurally characterized by spectral methods (FT-IR and photoluminescence), elemental analysis, thermal analysis (TG, DTG, DTA) and single crystal X-ray diffraction techniques. The synthesized complexes exhibit structural and dimensional diversity. In order to understand the potential of these complexes in gas adsorption and gas separation applications, atomically detailed simulations were performed. The antimicrobial properties of the complexes were also investigated by MIC (minimum inhibitory concentration) analysis to assess the potential of complexes in medical usage.

Experimental

Materials and physical measurements

All chemicals used were of analytical grade and were purchased commercially. The IR absorption spectra were recorded in the range of 400–4000 cm^{-1} by means of a Bruker Tensor 27 FT-IR spectrometer with KBr pellets. Elemental analyses for C, H and N were carried out at the TÜBİTAK Marmara Research Centre. Magnetic susceptibility measurements were performed using a Sherwood Scientific MXI model Gouy magnetic balance at room temperature. The decomposition enthalpies (ΔH, J mol^{-1}) of each stage were examined by differential scanning calorimetry (DSC) at a heating rate of 10 °C min^{-1} in a Seiko DSC 6200 (Exstar 6000, Seiko Instruments Inc.). The UV-vis spectra were obtained for the aqueous solution of the complexes (10^{-2} M) with a Lambda 35 UV-vis spectrometer in the range 900–190 nm.

Crystallographic analyses

Diffraction measurements were performed at 100 K on a Bruker Smart Apex CCD diffractometer using Mo Kα radiation (λ = 0.71073 Å). The structures were solved by direct methods using the program SHELXS-97[59] with anisotropic thermal parameters for all non-hydrogen atoms. All non-hydrogen atoms were refined anisotropically by full-matrix least-squares methods using SHELXL-97.[59] Molecular drawings were obtained by using Mercury.[60]

Details of the refinement are presented in Table 1; the crystallographic information files are deposited with the CCDC (887870–887874).

Calculation methods

In order to assess the potential of synthesized complexes in gas storage and gas separation applications, molecular simulations were performed. Grand Canonical Monte Carlo (GCMC)[61] simulations were used to compute single component adsorption of H_2 and CH_4 in all complexes. Rigid and solvent-free structures were used in molecular simulations. A number of studies in the past showed that several general purpose force fields such as UFF employed in adsorption simulations of coordination polymers give reasonable agreement with experiments,[62] therefore we used universal force field (UFF).[63] Spherical Lennard-Jones (LJ) 12–6 potentials were used to model H_2[64] and CH_4[65] molecules. Interactions between adsorbates (H_2 and CH_4) and adsorbents (complexes) were modeled using pair-wise interactions between adsorbate molecules and each atom in the complexes. Mixed-atom interactions were defined using the Lorenz–Berthelot mixing rules. The interactions with the atoms of complexes were

Table 1 Crystallographic data and structural refinement summary for **1–5**

	1	**2**	**3**	**4**	**5**
Chemical formula	$C_{17}H_{31}CuN_5O_4$	$C_{38}H_{50}N_{10}O_{10}Cu_2$	$C_{19}H_{23}N_5O_4Cd$	$C_{20}H_{42}Ag_2CuN_8O_{14}$	$C_{14}H_{18}CdCuN_2O_{14}$
FW/g mol^{-1}	433.01	933.97	497.84	933.93	614.26
Crystal system	Monoclinic	Monoclinic	Orthorhombic	Monoclinic	Monoclinic
Space group	$P2_1/n$	$P2_1/n$	$P2_12_12_1$	$C2/c$	$I2/a$
a/Å	12.996(5)	11.135(5)	13.536(3)	23.396(5)	16.435(5)
b/Å	22.878(5)	13.601(5)	9.938(4)	6.654(5)	7.076(5)
c/Å	13.696(5)	14.886(5)	16.885(6)	23.775(5)	20.060(4)
β/°	93.972(5)	96.368(5)	90.000	112.264(3)	107.658(5)
V/Å^3	4062(2)	2240.5(2)	2271.4(2)	3425.29(3)	2222.94(2)
Z	8	2	4	4	4
d_c/g cm^{-3}	1.416	1.384	1.456	1.811	1.841
μ (Mo Kα)/mm^{-1}	1.107	1.013	0.993	1.826	1.984
F(000)	1832	972	1008	1892	1228
Data collection					
Radiation (Å)	Mo Kα = 0.71069				
Theta min, max (°)	1.7, 26.5	2.4, 28.4	1.9, 28.4	3.1, 28.6	2.1, 35.4
Dataset	−16 → 15	−14 → 14	−18 → 16	−29 → 31	−26 → 21
	−28 → 28	−18 →18	−12 → 12	−8 → 8	−9 → 8
	−14 → 17	−19 →19	−17 → 22	−31 → 31	−18 → 22
Tot., uniq. data, R_{int}	35 184, 8419, 0.063	21 186, 5576, 0.062	15 988, 5559, 0.077	14 008, 4224, 0.054	7208, 2776, 0.038
Observed data [$I > 2\sigma(I)$]	4793	3261	3117	2683	2124
Refinement					
N_{ref}, N_{par}	8419, 487	5576, 286	5559, 266	4224, 221	776, 154
R, wR_2	0.0556, 0.1729	0.0470, 0.1150	0.0500, 0.1344	0.0631, 0.2180	0.0768, 0.2538
S	1.02	0.98	0.82	1.11	1.07
Min. and max. resd. dens. (e Å^{-3})	−0.70, 1.97	−0.35, 0.49	−0.81, 0.58	−2.43, 1.07	−1.60, 4.57

pretabulated on a 0.2 Å grid.[66] The conventional GCMC technique was used in this work to compute adsorption isotherms.[67] The temperature and fugacity of the adsorbing gases were specified and the number of adsorbed molecules at equilibrium was calculated. A cut-off distance of 13 Å was used for LJ interactions. Periodic boundary conditions were applied in all simulations. The size of the simulation box was set to 2 × 2 × 2 crystallographic unit cells. Simulations consisted of a total of 1 × 10^7 trial configurations, with the last half of the configurations used for data collection. A configuration is defined as an attempted translation, or creation, or deletion of an adsorbate molecule. For the case of mixture simulations, there is also an attempted swap of the particle species of a molecule. For mixture simulations, equimolar CH_4–H_2 mixtures were considered.

Antimicrobial activities

The antimicrobial activities (MIC values) of complexes were tested against standard bacterial strains *Staphylococcus aureus* ATCC6535, *Bacillus cereus* ATCC7064, *Escherichia coli* ATCC25922, *Pseudomonas aeruginosa* ATCC27853, one yeast *Candida albicans* ATCC10231 and some clinical isolates methicillin resistant *S. aureus*, *E. coli*, *Acinetobacter baumannii, Morganella morganii*, *Enterobacter aerogenes* (isolated by Faculty of Medicine, Ondokuz Mayıs University) by using broth dilution method. The complexes were dissolved in double distilled water at proper concentration. For the broth dilution method, cultures were grown in 5 mL nutrient broth (Merck) at 37 °C for 18 h in shaking at 175 rpm. Bacterial and yeast cells were suspended in 50 mL nutrient broth at a concentration of approximately 5 × 10^5 cells per mL by matching with 0.5 McFarland turbidity standards. Nutrient broth containing microorganisms (1 mL) were transferred to test tubes, to which were added the complexes, and a 2-fold serial dilution was made. All the test cultures were grown at 37 °C in an incubator. The incubation period was 24 h for bacterial strains and fungal strains. The minimum inhibitor concentration, at which no growth was observed, was taken as the MIC value (μg mL^{-1}).

Preparation of the complexes

{[Cu(μ-pydc)(dmpen)$_2$]}$_n$ (1). 10 mL dimethylformamide solution of pydcH_2 (1.00 g, 5.98 mmol) was treated with metallic copper (0.38 g, 5.98 mmol) under stirring at 80 °C. The solution immediately precipitated and was stirred for 1 h at 80 °C. Then the dmpen ligand (1.22 g, 11.96 mmol) in water (10 mL) was added dropwise to this solution. The clear solution was stirred for 2 h at 50 °C and then cooled to room temperature. Dark blue crystals were formed and washed with 10 mL of water and then dried in air. Yield: 33% (based on Cu) for **1**. Anal. found: C, 47.22; H, 7.27; N, 16.14%. Calcd. for: $C_{17}H_{31}CuN_5O_4$, C: 47.15; H: 7.22; N: 16.17%. IR (cm^{-1}, KBr): ν(CH), 3273 w, 3215 w, 3130 w; ν(NH), 2954 m; 2904 w; 2868 m ν_{as}(COO), 1645 sh, 1587 vs; ν(C=N), 1458 w; ν_s(COO), 1380 vs; $\Delta\nu$, 207.

[Cu$_2$(μ-pydc)$_2$(emim)$_4$]·2H$_2$O (2). This complex was obtained in a similar way to that of **1**, but dmpen was replaced by emim ligand (1.32 g, 11.96 mmol). Green crystals were formed and washed with 10 mL of water and then dried in air. Yield: 48% (based on Cu) for **2**. Anal. found: C, 48.87; H, 5.42; N, 15.04%. Calcd. for: $C_{38}H_{50}N_{10}O_{10}Cu_2$, C: 48.85; H: 5.42; N: 15.00%. IR (cm^{-1}, KBr): ν(H$_2$O), 3491 w; ν(NH), 3158 s; ν(CH), 3069 w,

2974 w, 2750 w, 2634 w; ν_{as}(COO), 1671 vs, 1586 vs; ν(C=N), 1478 m; ν_s(COO), 1393 vs, 1365 vs; $\Delta\nu$, 278 and 221.

$[Cd(\mu\text{-pydc})(emim)_2]_n$ (3). This complex was obtained in a similar way to that of **2**, but metallic copper was replaced by $Cd(CH_3COOH)_2{\cdot}2H_2O$ (1.59 g, 5.98 mmol). Colorless crystals were formed and washed with 10 mL of water and then dried in air. Yield: 54% (based on Cd) for **3**. Anal. found: C, 45.78; H, 4.71; N, 14.12%. Calcd. for: $C_{19}H_{23}N_5O_4Cd$, C: 45.84; H: 4.66; N: 14.07%. IR (cm^{-1}, KBr): ν(NH), 3142 s; ν(CH), 3087 w, 2752 w, 2625 w, 2625 w; ν_{as}(COO), 1623 vs, 1576 vs; ν(C=N), 1466 vs; ν_s(COO), 1404 vs, 1378 vs; $\Delta\nu$, 219 and 198.

$[Cu(en)_2(H_2O)_2][Ag_2(pydc)_2(\mu\text{-en})]{\cdot}6H_2O$ (4). The complex was synthesized in three stages. First 10 mL DMF solution of $pydcH_2$ (1.00 g, 5.98 mmol) was treated with KOH (0.67 g, 11.96 mmol) and metallic copper (0.38 g, 5.98 mmol) under stirring at 80 °C. The resulting solution was left to evaporate slowly in the dark at room temperature for several weeks. The dark blue crystals of $K_2[Cu(pydc)_2]{\cdot}3H_2O$ were formed and washed with 10 mL of water and then dried in air. In the second stage a solution of $K_2[Cu(pydc)_2]{\cdot}3H_2O$ (0.50 g, 0.956 mmol) in water (20 mL) was added dropwise with stirring to a solution of $AgNO_3$ (0.32 g, 1.91 mmol) in water (20 mL). The solution immediately precipitated and was stirred for 1 h at 80 °C. The precipitation of $Ag_2[Cu(pydc)_2]{\cdot}H_2O$ product was filtrated off and dried in air. In the last stage uncharacterized light blue $Ag_2[Cu(pydc)_2]{\cdot}H_2O$ was added to 10 mL water and the mixture was stirred for 4 h at 50 °C and then en (0.074 g, 1.2 mmol) in water (25 ml) was added to the mixture to give a clear solution. The resulting solution was left to evaporate slowly in the dark at room temperature for several weeks until violet crystals were formed, which were washed with 10 mL of water and then dried in air. Yield: 67% (based on Cu) for **4**. Anal. found: C, 26.69; H, 4.77; N, 12.41%. Calcd. for: $C_{20}H_{42}Ag_2CuN_8O_{14}$, C: 26.75; H: 4.71; N: 12.48%. IR (cm^{-1}, KBr): ν(H_2O), 3358 m; ν(CH), 3294 s, 3238 s; ν(NH), 2975 m; 2953 m; 2886 m; ν_{as}(COO), 1593 sh, 1571 vs; ν(C=N), 1454 w; ν_s(COO), 1382 vs; $\Delta\nu$, 211.

$\{[Cd(H_2O)_4Cu(\mu\text{-pydc})_2]{\cdot}2H_2O\}_n$ (5). This complex was obtained in a similar method to that of **4**, but $AgNO_3$ was replaced by $Cd(CH_3COOH)_2{\cdot}2H_2O$ (1.59 g, 5.98 mmol). Sky-blue crystals were formed and washed with 10 mL of water and then dried in air. Yield: 21% (based on Cd) for **5**. Anal. found: C, 27.37; H, 2.95; N, 4.56%. Calcd. for: $C_{14}H_{18}CdCuN_2O_{14}$, C, 27.31; H, 2.89; N, 4.49%. IR (cm^{-1}, KBr): ν(H_2O), 3456 m; ν(CH), 3201 w, 3156 w; ν_{as}(COO), 1644 vs, 1588 vs; ν(C=N), 1454 m; ν_s(COO), 1395 m, 1367 m; $\Delta\nu$, 249, 221.

Result and discussion

Crystal structures

The relevant crystal data and experimental conditions with the final parameters are summarized in Table 1. The selected bond lengths and angles together with the hydrogen bonding geometry are tabulated in the relevant sections. The molecular structures of the compounds with atom numbering scheme are shown in the relevant sections .

$[Cu(\mu\text{-pydc})(dmpen)_2]_n$ (1). $[Cu(\mu\text{-pydc})(dmpen)_2]_n$ (**1**) crystallizes in monoclinic $P2_1/n$ space group. The asymmetric unit of the complex contains two independent $[Cu(\mu\text{-pydc})(dmpen)_2]$ unit (Fig. 1a). The nitrogen atom of pydc ligand was not coordinated to the Cu(II) center in **1** (Scheme 1) and this situation is seen in the literature for the first time. The unexpected non-coordination of the pyridine nitrogen atom in **1** may arise from the steric effect of the methyl groups within the 1,3-diamino-2,2-dimethylpropane ligand that occupy a certain amount of space around the pyridine nitrogen atom (Fig. S1, ESI†). In $[Cu(\mu\text{-pydc})(dmpen)_2]_n$ (**1**), the nitrogen atoms of dmpen ligands coordinated to the copper(II) ions to form equatorial planes around the metal centers and one of the carboxylate groups of pydc ligands bonded to the Cu(II) ions by their O1 and O5 carboxylate oxygen atoms in the axial positions. The mononuclear units at $\pm1/2 + x$, $1/2 - y$, $\pm1/2 + z$ completed the coordination around the Cu(II) center using by their O3 and O8 carboxylate oxygen atoms of pydc ligand and

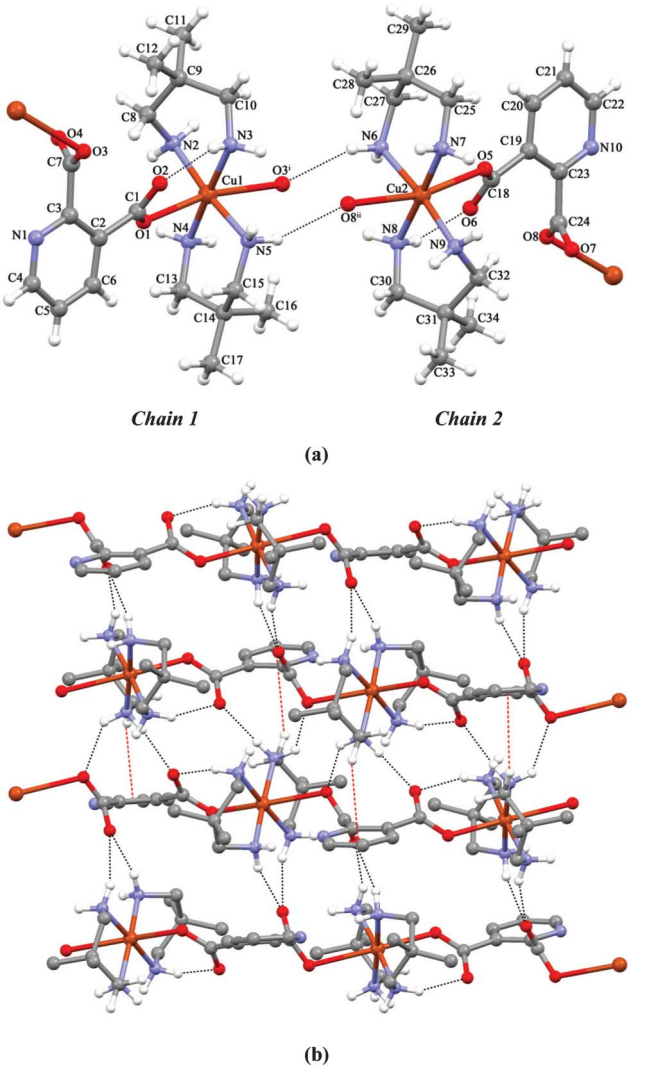

Fig. 1 (a) View of the asymmetric unit of **1** containing two different chains with atom-labelling scheme and (b) supramolecular N–H···O and C–H···π interactions between two chains in **1**.

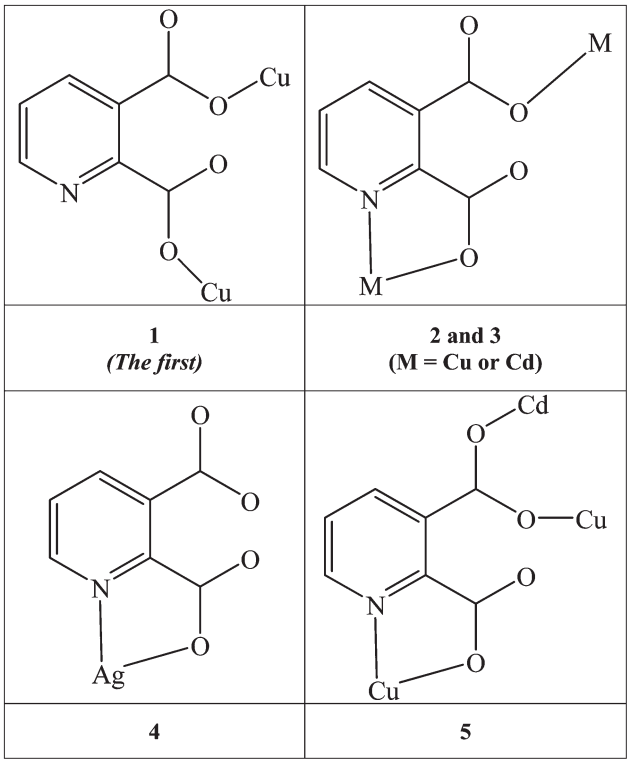

Scheme 1 Coordination modes for the pydc ligand in **1–5**.

arrange in order to form a 1D polynuclear structure by the two-fold screw axis, so the mononuclear units go at $x + n$, y, $z + n$ and $\pm 1/2 + x + n$, $1/2 - y$, $\pm 1/2 + z + n$ symmetries (n is an integer) to compose two infinite different one dimensional chains along the [100] and [001] directions (Fig. 1b) and the pydc ligands act as bridge between the symmetry related [Cu(dmpen)$_2$] complex units.

The coordination bond lengths in the polymers, for Cu1–O1, Cu1–O3^{i}, Cu2–O5 and Cu2–O8^{ii} are found to be 2.388, 2.638, 2.348 and 2.597 Å, respectively ((i) $1/2 + x$, $1/2 - y$, $1/2 + z$ and (ii) $-1/2 + x$, $1/2 - y$, $-1/2 + z$) and Cu–N$_{dmpen}$ bond lengths were in the range of 2.007(4) to 2.032(3) Å (Table S1, ESI†). The shortest Cu–Cu separation was found to be 6.114 Å between the polynuclear chains. In **1**, the pyridine rings of pydc are nearly planar with the largest deviation from the plane being that of atom C6 [0.006(5) Å] in chain 1 and C20 in chain 2 [0.008(5) Å] and the two pyridine ring planes in the asymmetric unit are nearly parallel to each other, with the angle between the two planes being 2.055(8)°. The angle between the symmetry related (i and ii) pyridine rings of pydc ligands was 18.592(8)° in chain 1 and 14.669(9)° in chain 2. The carboxylate groups were not in the pyridine ring planes. The angle between the pyridine ring planes and carboxylate groups were 41.86 and 67.35° for (O1–C2–O2) and (O3–C7–O4), respectively, in chain 1, and 41.29 and 66.53° for (O5–C18–O6) and (O7–C24–O8), respectively, in chain 2. The nearest distance between the aromatic rings of pydc ligands in polymer chains is found to be 5.235(3) Å at $\pm 3/2 + x$, $1/2 - y$, $\pm 1/2 + z$ and 7.765 Å in the asymmetric unit. The C15 atom of dmpen ligand in the asymmetric unit showed the C–H···π interaction using its hydrogen atom with the aromatic ring center of pydc ligand at (ii) $-1/2 + x$, $1/2 - y$, $-1/2 + z$ to bond the two polymer to each other. In **1**, the N2, N3 and N4 atoms act as hydrogen bond donors *via* one of their hydrogen atoms with the N1^{i}, O2, and O4^{i}, respectively, to form intrachain hydrogen bonds (Fig. 1b and Table S6, ESI†). In addition to these interchain hydrogen bonds, the N5 atom of the dmpen ligand in **1** acts as a hydrogen bond donor *via* its hydrogen atoms to O6^{ii} and O8^{ii} atoms of pydc ligand. In chain 2, the N7, N8 and N9 atoms act as hydrogen bond donors *via* their one of hydrogen atoms with the O7^{iii}, O6, and N10^{ii}, respectively, to form intrachain hydrogen bonds. The remaining hydrogen atoms of these donors composed inter-polymer hydrogen bonds to bond polymers to each other with O4^{iv} and O2^{i} atoms and the N6 atom of the dmpen ligand in chain 1 acting as a hydrogen bond donor *via* its hydrogen atoms to O2^{i} and O3^{i} atoms of pydc ligand (Fig. 1b, Table S6, ESI†). All of the interchain hydrogen bonds link the chains to each other to form three dimensional network.

[Cu$_2$(μ-pydc)$_2$(emim)$_4$]·2H$_2$O (2). The complex [Cu$_2$(μ-pydc)$_2$(emim)$_4$]·2H$_2$O (**2**) crystallizes in the monoclinic $P2_1/n$ space group. The asymmetric unit of the complex contains a Cu(II) ion which lies on an inversion center, a pyridine-2,3-dicarboxylate dianion (pydc), two neutral 2-ethyl-5-methylimidazole (emim) ligands and a hydrate water (Fig. 2a). The crystal structure of **2** showed the 2-ethyl-4-methylimidazole ligands changed to 2-ethyl-5-methylimidazole ligands by proton transfer on the nitrogen atoms of the imidazole rings during the complexation reaction. We reported similar proton transfer reactions in imidazole rings in our previous studies.[68,69] The two [CuO$_2$N$_3$] coordination systems in the dinuclear structure are formed by two oxygen and one nitrogen atoms from two pydc ligands [Cu1–O1 = 1.986 (2), Cu1–O3^{i} = 2.191 (2) and Cu1–N1 = 2.017 (2) Å, (i) $-x$, $-y$, $-z + 1$] and two N atoms from two emim ligands [Cu1–N2 = 1.987 (2) and Cu1–N4 = 1.979 (2) Å] in the asymmetric unit (Table S2, ESI†). The dinuclear structure is completed with the asymmetric unit at $-x$, $-y$, $-z + 1$ *via* bonding the remaining carboxylate oxygen (O3 and O3^{i}) to the Cu(II) ion to form the first identified dinuclear structure for Cu(II) complexes of pydc ligand. So the two pydc anions act as a bridge between two [Cu(emim)$_2$] complex units (Fig. 2b). A similar dinuclear complex was reported only for a cobalt complex of pydc.[70] The bond length of the Cu–O bonds (1.984 and 2.191 Å) and Cu–N$_{pydc}$ (2.016 Å) are comparable to those of other some pydc complexes (Cu–O = 1.986 (2)–2.191 (2) and Cu–N$_{pydc}$ = 1.980 (2)–2.017 (2) Å) in the literature.[32,71–75] The bond lengths were compared with the dinuclear cobalt complex and some polynuclear copper complexes which contain acceptably similarly orientated pydc ligands. In complex **2**, the pyridine rings of pydc are nearly planar with the largest deviation from the plane being that of atom C3 [0.005(3) Å] and the two pyridine ring planes are parallel to each other, with the distance and angle between the two planes being 4.097(2) Å and 0°, respectively. One of the carboxylate groups (O1–C2–O2) was nearly in the pyridine ring plane with an angle of 4.85° and the other carboxylate group (O3–C4–O4) was nearly perpendicular to the pyridine ring plane with an angle of 86.74°. The bond lengths and angles of O1–C1–O2 reflect the π electron delocalization through these

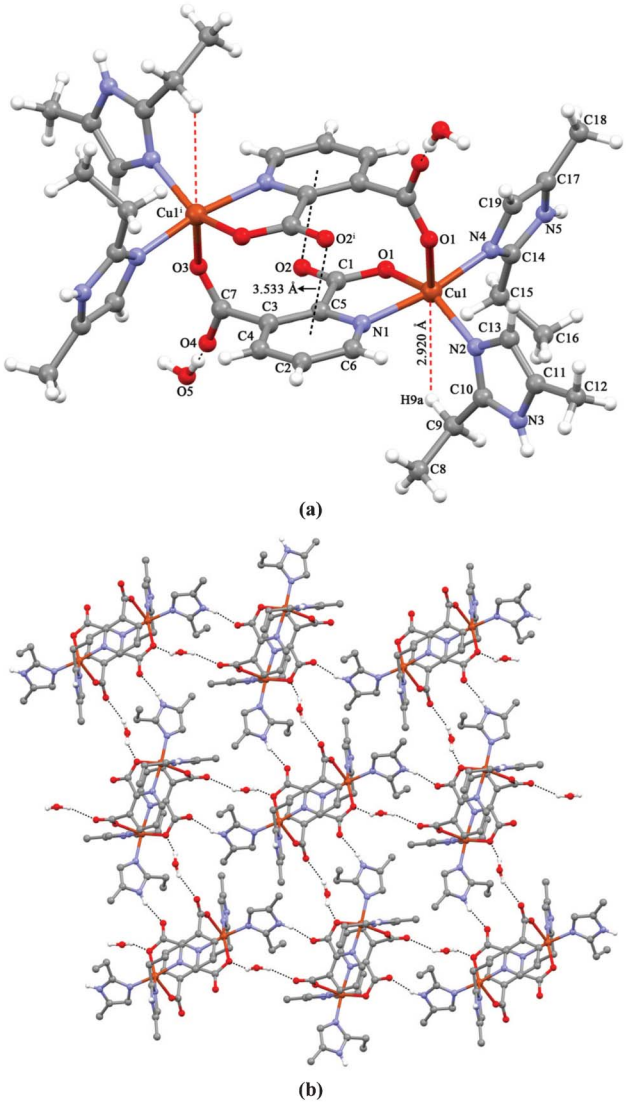

Fig. 2 (a) View of the asymmetric unit of **2** with atom-labelling scheme and (b) hydrogen bonding interactions between two dinuclear units in **2** (symmetry code: (i) 1 − *x*, 1 − *y*, 2 − (*z*).

three atoms. The distance and angles between the five membered ring plane formed by coordination and symmetry related pyridine ring planes of pydc were measured as 3.492(11) Å and 6.00(12)°, respectively. There were also C–O···π interactions between the uncoordinated carboxyl oxygen (O2) and aromatic rings of pydc [3.535(3) Å] (Fig. 2b). Similar C–O···π interactions were reported as 3.163 and 3.239 Å previously in two polynuclear copper(II) complexes of pydc.[32,71]

The most striking property of complex **2** is the presence of the rare C–H···Cu type hydrogen bonding interactions. The distance of C9–H9A and C15–H15A atoms of the ethyl group of emim ligands and Cu(II) centers are 2.920(5) and 2.969(5) Å, respectively. The angles are 116.37(5)° for C9–H9A···Cu and 112.52(5)° for C15–H15A···Cu. These results indicated an interaction between the C–H and Cu(II) center (Table S7, ESI†). This X–H···M type interaction, named as agostic or anagostic interactions, was first suggested in 1972 by Roe *et al.*[76] The literature survey shows that the X–H···M angle is around 110–170° for anagostic interactions, which reflects largely electrostatic interactions and around 90–140° for agostic interactions suitable with 3-center–2-elecron interactions.[77] The bond lengths and angles indicated that anagostic interactions are present in **2**. The anagostic interactions were first explored for pydc or emim complexes in this work. The C19–H19 of an emim ligand formed intramolecular hydrogen bonds with the O3^{i} atom of pydc ligand at ((i) $-x$, $-y$, $-z+1$). The dinuclear complex units bonded to each other along the *c* axis by the O5–H5w···O1, C2–H2···O5^{i} and O5–H5w′···O4^{iii} intermolecular hydrogen bonds, so the hydrated water molecules act as a bridge between the dinuclear complexes (Table S7, ESI†). The complex unit lying at the $-x$ (+1/2 and $-1/2$), $y+1/2+n$, $-z+1/2$ and *x* (+1/2 and $-1/2$), $-y+1/2+n$, $z+1/2$ symmetries (*n* is an integer) that formed a dinuclear complex bonded the dinuclear complex units to each other along the *x* and *y* axis with the N3–H3···O4^{ii}, and N5–H5···O2^{iii} intermolecular hydrogen bonds (Fig. S2, Table S7, ESI†). So these intermolecular hydrogen bonds formed three dimensional network.

[Cd(μ-pydc)(emim)$_2$]$_n$ (3). The X-ray crystallographic analysis shows that **3** crystallizes in the orthorhombic space group $P2_12_12_1$ and has an infinite 1D chain structure. As shown in Fig. 3a, a crystallographically independent Cd(II) ion is surrounded by a distorted octahedral geometry with two emim ligands and three oxygen and one nitrogen atoms from two pydc ligands (Table S3, ESI†). The equatorial plane of the octahedral geometry is provided by one nitrogen atom from emim, one nitrogen atom from pydc ligand and two oxygen atom from different two pydc ligands. The axial position is occupied by a carboxylate oxygen atom from pydc and a nitrogen atom from the emim ligand. The pydc ligand is coordinated to two Cd(II) ions in a bis(bidentate) mode with its one nitrogen atom of the pyridine ring and three oxygen atoms of the carboxylate groups to form a one-dimensional chain.

The crystal packing of the complex is a composite of C–H···π and hydrogen bonding interactions (Table S8, ESI†). The adjacent 1D chains extend into a 3D supramolecular network by N5–H5···O4 and N9–H9···O3 hydrogen bonds and C–H···π interactions (Fig. 3b and Fig. S3a, ESI†). Furthermore, there is an interchain C–H···π interaction between C–H groups (C13–H13b, C16–H16a and C16–H16c) and imidazole (Cg1: N4–C14–C15–N5–C17; H13b···Cg1 = 3.039, H16c···Cg1^{i} = 3.218 Å, (i) $2-x$, $-1/2+y$, $1.5-z$) or pyridine (Cg2: N1–C1–C2–C3–C4–C5, H16A···Cg2^{i} = 2.921 Å) (Fig. S3b, ESI†).

[Cu(en)$_2$(H$_2$O)$_2$][Ag$_2$(pydc)$_2$(μ-en)]·6H$_2$O (4). Complex **4** crystallizes in the monoclinic *C*2/*c* space group. The asymmetric unit of the complex contains a Cu(II) ion, an ethylenediamine (en) ligand and an aqua ligand which lie on a crystallographic centre of symmetry ($-x$, *y*, 3/2 − *z*), a silver(I) ion, a pyridine-2,3-dicarboxylate dianion (pydc) and a half en ligands and three hydrate waters lying on a crystallographic centre of symmetry (1/2 − *x*, 1/2*y*, 1 − *z*) (Fig. 4). The compound contains two complex units which are diaquabisethylenediamincopper(II), [Cu(H$_2$O)$_2$(en)$_2$] and μ-ethylenediamine bis(pyridine-2,3-dicarboxylatosilver(I)), [Ag(pydc)$_2$(μ-en)], and six hydrate water molecules.

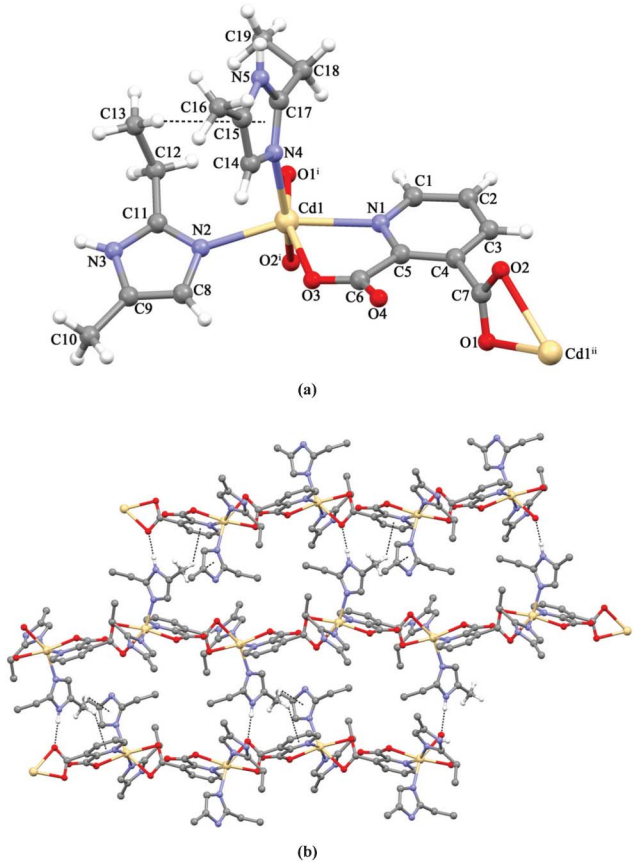

Fig. 3 (a) View of the asymmetric unit of **3** with atom-labelling scheme and (b) hydrogen bonding and interchain C–H···π interactions in **3** (symmetry codes: (i) −1/2 + *x*, 1.5 − *y*, 1 − *z*, (ii) 1/2 + *x*, 1.5 − *y*, 1 − *z*).

One of the most striking features of **4** is that it has two en ligands in different coordination manners. One of them acts as a bidentate ligand and is coordinated to the Cu(II) ion and the other one acts as bridged ligand between the two Ag(I)–pydc units. The two en ligands in different manners were seen in this work for the first time (Fig. S4a, ESI†). The two en ligands occupied the equatorial positions of octahedral around the Cu(II) center and aqua ligands coordinated to Cu(II) through the axial positions to complete an octahedral geometry (Cu1–O8 = 2.614(5), Cu1–N3 = 2.004(6) and Cu1–N4 = 2.012(7) Å) (Table S4, ESI†). The ethylenediamine and aqua ligands were oriented by a symmetry operation in *cis*- and *trans*-forms, respectively. To form the Ag(I)–pydc parts of the compound, the pydc ligands bonded to Ag(I) ions *via* their pyridine nitrogen and an oxygen atom of the carboxylate groups, which is in the *ortho* position. The en ligand acted in a bridging manner between the two Ag(I)–pydc parts to form an en bridged dinuclear $[Ag_2(pydc)_2(\mu\text{-en})]$. The bond lengths were measured as 2.451(5), 2.178(5) and 2.158(5) Å for O1–Ag1, N1–Ag1 and N2–Ag1, respectively.

The pyridine rings of pydc are nearly planar with the largest deviation from the plane being that of atom C6 [0.007(6) Å]. The two pyridine ring planes in the dinuclear structure are parallel to each other and the distance and angles between the two planes are 1.189 Å and 0°, respectively. One of the carboxylate groups (O1–C2–O2) was nearly in the pyridine ring plane with the angle of 3.26° and the other carboxylate group (O3–C7–O4) was nearly perpendicular to the pyridine ring planes with an angle of 85.39°.

The complex units in the compound showed interesting arrangements. $[Ag(pydc)_2(\mu\text{-en})]$ complex units related by symmetry were bonded to each other by Ag–Cg secondary interactions (3.445 and 3.377 Å; Cg refers to the center of gravity of the pydc rings) and C–H···O and N–H···O hydrogen bonds to form $[Ag(pydc)_2(\mu\text{-en})]$ complex layers through the *b* axis (Fig. S4b, ESI†).

The independent $[Cu(H_2O)_2(en)_2]^{2+}$ complex ion units settled between the layers by symmetry and bonded the layers to each other by using their aqua ligands and the NH_2 parts of en ligands to form N–H···O and O–H···O hydrogen bonds with the uncoordinated carboxylate oxygens of pydc ligands of $[Ag(pydc)_2(\mu\text{-en})]$ complex units (Fig. S5, ESI†). So, the independent $[Cu(H_2O)_2(en)_2]^{2+}$ complex units bridged the dinuclear $[Ag(pydc)_2(\mu\text{-en})]$ complex units that form layers along the *a*, *b* and *c* axis by symmetry to form three dimensional supramolecular networks which have solvent accessible voids along the *b* axis (Fig. 5). Interestingly, in these voids, the crystal water molecules are bonded to each other by hydrogen bonds to form the pentagonal water rings. In the infinite water tape involving cyclic pentamer water clusters extended along the *c*-axis with a T(5)2 motif, which has been reported rarely so far[78] (Fig. S6a, ESI†). The geometric

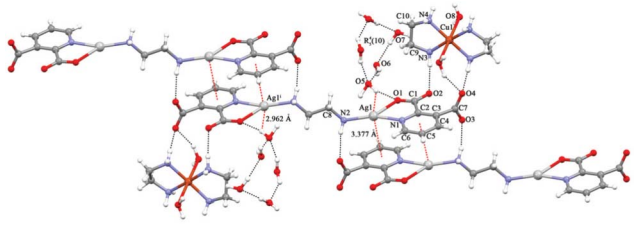

Fig. 4 Perspective view of supramolecular interactions (Ag···π, hydrogen bond and O–H···Ag) of the **4** with atom-labelling scheme (symmetry code: (i) 1/2 − *x*, 1/2 − *y*, 1 − *z*).

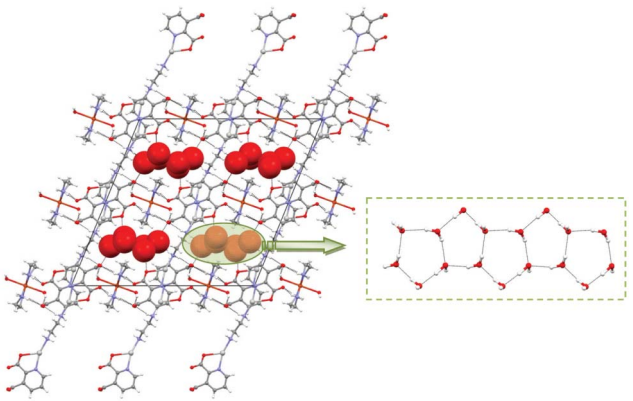

Fig. 5 Three dimensional supramolecular network of **4** which have 1D T5(2) water tape inside the voids along the *b* axis.

parameters of the 1D water cluster are summarized in Table S8, ESI.† The average O···O distance in the water tape is 2.832 Å, which is slightly shorter than that observed in liquid water (2.854 Å) and similar to those in the ice II phase (2.77–2.84 Å). The water rings also act as hydrogen bond donors to carboxylate oxygens of pydc ligands of [Ag(pydc)$_2$(μ-en)] complex units (Fig. S6b, ESI†). The bridged en ligands act as hydrogen bond donors to the T(5)2 water cluster by using one hydrogen atom of each of their two NH_2 parts and so each of the dinuclear [Ag(pydc)$_2$(μ-en)] complex units act as a bridge between the six infinite water chains lying along the *b* axis.

More interestingly, besides the classical hydrogen bonds, an intermolecular O–H···Ag close interaction between H5A in crystal water molecules and Ag1 centers have been observed. The Ag1···H5A, Ag1···O5 distances and Ag1···O–H5A angle are 2.962, 3.687 Å and 139.82°, respectively and this intermolecular O–H···Ag close interaction is well described as being weak intermolecular O–H···Ag hydrogen bonding.[79]

Crystal structure of {[Cd(H$_2$O)$_4$Cu(μ-pydc)$_2$]·2H$_2$O}$_n$ (5). Complex **5** crystallizes in the monoclinic *I*2/*a* space group. The asymmetric unit of the complex contains a Cu(II) ion, a Cd(II) ion, a pyridine-2,3-dicarboxylate dianion (pydc), two aqua ligands and a crystal water molecule (Fig. 6a). In the literature there are some polynuclear Cu(II) complexes of pydc ligands formed with only pydc ligands. In this report the pydc ligands act as bidentate ligands using their pyridine N and a carboxylate O in the *ortho* position and act in a bridging manner using one of their carboxylate O in the *meta* position to form a monometallic 1D polynuclear structure. Only one of the two carboxylate oxygens was used to coordinate and to form a polynuclear arrangement. This work is the first example of polynuclear pydc compounds having different metals (3d–4d) that are in different coordination spheres or three carboxylate oxygen atoms used to form a 2D polynuclear arrangement (Fig. 6b).

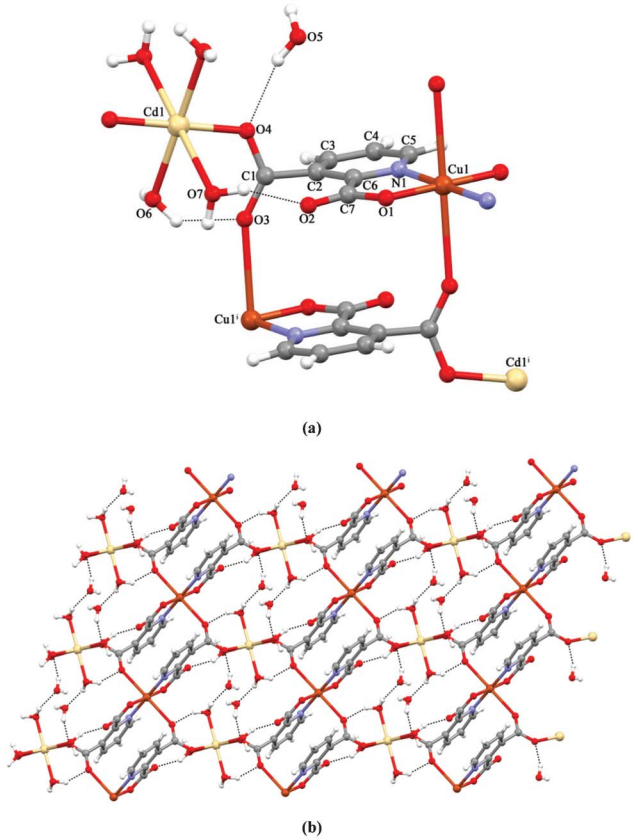

Fig. 6 (a) View of the asymmetric unit of **5** with atom-labelling scheme (b) 2D sheet structure containing hydrogen bonding interactions in **5** (symmetry code: (i) *x*, −1 + *y*, *z*).

In **5**, pydc ligands bonded to Cu(II) ion using their pyridine N and carboxylate O in the *ortho* position to compose the equatorial plane of octahedron around the copper ion, similar to the literature examples. The other carboxylate oxygens (O3 and O4) in the *meta* position were free to bond in a bridging manner. Meanwhile, one of the carboxylate oxygens (O3) in the *meta* position coordinated to a symmetry related Cu(II) through the axial position to form a 1D [Cu(pydc)] polynuclear complex along the *c* axis, like the literature examples, as in different literature examples the other carboxylate oxygens (O4) in the *meta* position bonded to Cd(II) coordinated by four aqua ligands to form polymeric structure along the *b* axis. So, the Cd(II) ions act as a bridge bonding 1D chains to each other by bonding to the O4 atom of pydc ligands in Cu(II)–pydc polymers to form a two dimensional network.

The Cu atoms displaying distorted octahedral geometry were bonded to two pyridine N atoms (Cu1–N1 = 2.134 Å) and two O4 atoms of the carboxylate groups in the pyridine *ortho* positions (Cu1–O1 = 1.700 Å) which form the equatorial plane (Table S5, ESI†). The pydc ligands also bonded to Cd(II) ion by the O4 atoms of the carboxylate groups in the pyridine *meta* positions (Cd1–O4 = 1.946(4) Å) to form the complex polymer chain. The distorted octahedral geometry around the cadmium(II) centers was completed by the symmetry related aqua ligands (Cd1–O6 = 2.291 and Cd1–O7 = 2.797 Å). The O3 atoms of the carboxylate group in the pyridine *meta* positions bonded to the Cu1^{i} atom of adjacent polymer (Cu1–O3 = 2.734, (i) *x*, −1 + *y*, *z*). The distorted octahedral geometry around the Cu(II) atom in the asymmetric unit was completed by the O3 atoms of adjacent polymers at *x*, 1 + *y*, *z* and 1 − *x*, 1 − *y*, 1 − *z*.

The pyridine rings of pydc were nearly planar with the largest deviation from the plane being that of atom C2 [0.031(8) Å] and the two pyridine ring planes in the polymer were parallel to each other (0°) and the distance between the nearest two centers of phenyl rings was measured as 5.449(5) Å. The one of carboxylate group (O1–C7–O2) was nearly in the pyridine ring planes with an angle of 4.54° and the other carboxylate group (O3–C1–O4) was nearly perpendicular to the pyridine ring planes with an angle of 81.56°. We also found C–O···π interactions between the pydc ring and uncoordinated carboxylate oxygens with lengths of 3.711(8) Å.

All of the aqua ligands coordinating to Cd(II) ion and crystal water lying between the Cu(II)–pydc polymer chains act as hydrogen bond donors *via* one of their hydrogen atoms to the carboxylate oxygens of pydc ligands. Using the other hydrogen atom (H6A) the O6 of aqua ligands also formed hydrogen bonds with the O5 atom of crystal water at *x*, −1 + *y*, *z* (Table S9, ESI†). The O5 atoms of crystal waters also formed hydrogen bonds with the O4 atom of aqua ligands and so act as

bifurcated hydrogen bond donors. So the crystal waters and aqua ligands coordinating to Cd(II) ions formed metallo–water clusters lying parallel to the *b* axis.

Computational results

We examined gas adsorption properties of complexes to understand their potential in storage applications. Fig. 7 represents the single component adsorption isotherms of H_2 in all complexes at 77 and 298 K. The scatters are the results from GCMC simulations whereas the lines are the single component adsorption isotherm fits. At 298 K, H_2 is below saturation in all complexes and gas uptake increases as the pressure increases. At 77 K, except complex **1**, all complexes are saturated with H_2. Fig. 7 shows that complexes **2–5** can be potential candidates for H_2 storage. Since CH_4 has a larger kinetic diameter than H_2, CH_4 can only be adsorbed into the pores of two structures, **4** and **5**. Fig. 8 shows single component and equimolar binary mixture adsorption isotherms of CH_4 and H_2 in these complexes. As should be expected from the single component isotherms, adsorption favors CH_4 over H_2 in the mixture since the more strongly adsorbing CH_4 molecules exclude H_2 molecules in the pores. It is obvious from Fig. 8 that the amount of adsorbed gas in the mixture is smaller than the amount of adsorbed gas in the single component case due to the competitive adsorption between two gas species. In addition to mixture GCMC simulations, we also predicted mixture adsorption isotherms using a theoretical approach. Ideal Adsorbed Solution Theory (IAST)[80] is a well-developed technique to describe adsorption equilibria for components in a gaseous mixture, using only data for the pure component adsorption equilibria at the same

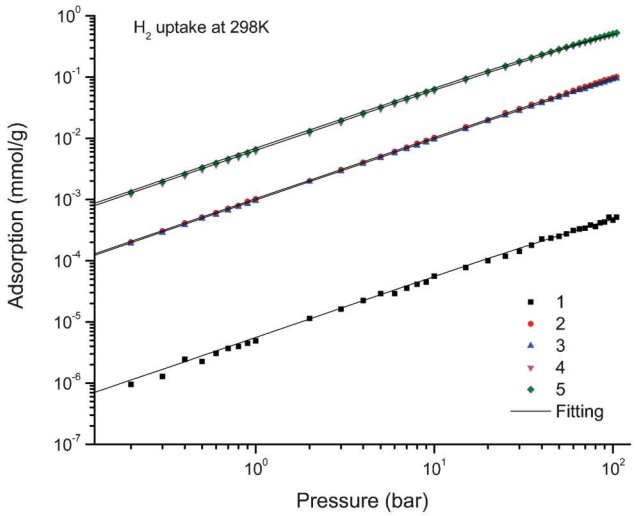

(a)

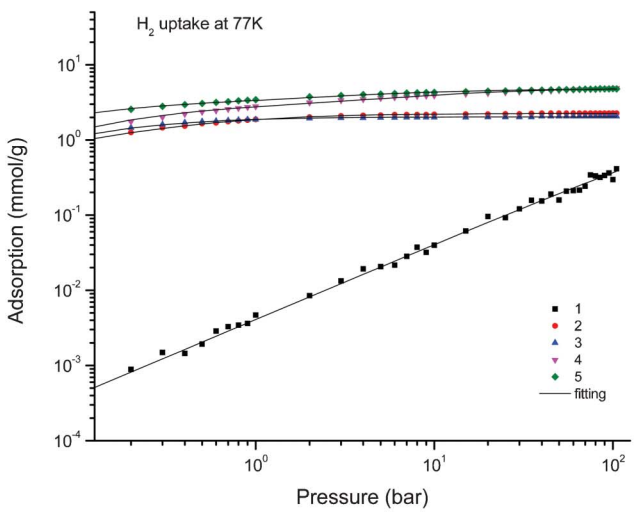

(b)

Fig. 7 Adsorption isotherms for H_2 at 77 K (a) and 298 K (b).

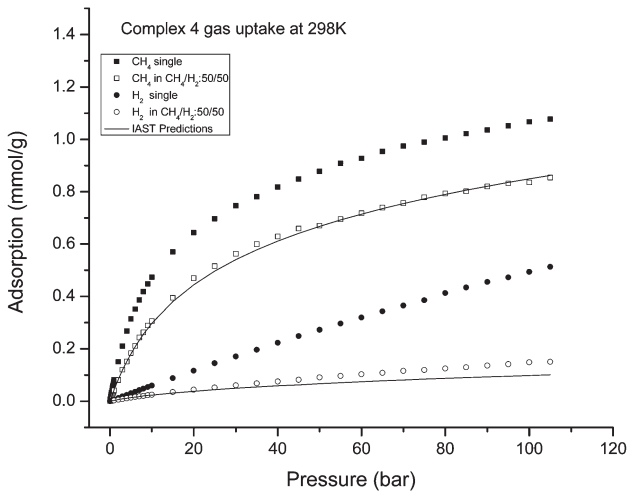

(a)

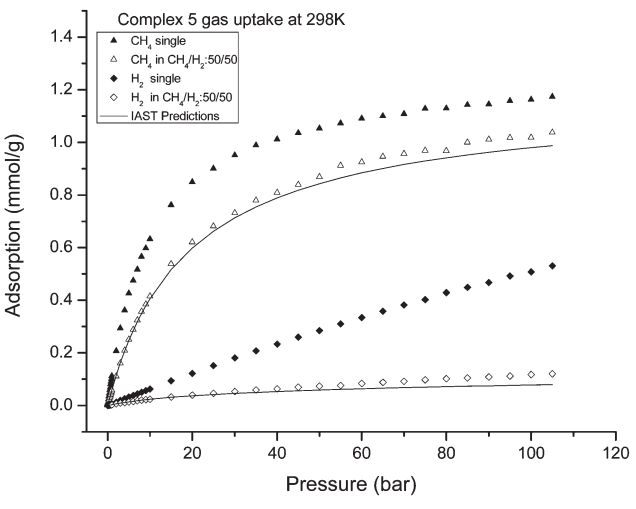

(b)

Fig. 8 Adsorption of CH_4 and H_2 in complexes **4** (a) and **5** (b) at 298 K.

temperature and on the same adsorbent. This theory is known to give accurate results in many nanoporous materials except in materials characterized by strong energetic or geometric heterogeneity.[81] Practical application of IAST requires that the functional form of the single component isotherms must be specified. In order to apply IAST, single component adsorption isotherms of CH_4 and H_2 were fitted using a dual site Langmuir isotherm and these fits were shown as continuous lines in Fig. 8. The predictions of IAST were found to be in a good agreement with the mixture GCMC simulations. This result indicates that IAST can be used to predict mixture adsorption accurately in the synthesized materials. A good indication of the ability for separation is the adsorption-based selectivity of a porous material for different components in the mixtures. The adsorption-based selectivity for CH_4 relative to H_2 is defined as $S_{CH_4/H_2} = (x_{CH_4}/x_{H_2})/(y_{CH_4}/y_{H_2})$, where x and y are the molar fractions of the adsorbed and bulk phase, respectively. The CH_4 adsorption selectivities of complexes **4** and **5** were found to be 12 and 17, respectively, at 10 bar and 298 K. This result suggests that these materials are potential candidates for CH_4–H_2 separation applications.

Complexes **4** and **5** are found to adsorb more H_2 compared to the complexes **1–3**. This can be explained by the following discussion: complex **5** is a 2D coordination polymer and it extends to 3D due to London interactions. The 2D interlayer space in the 3D supramolecular structure can be responsible for the high amount of H_2 adsorption in complex **5**. In complex **4**, a 1D structure is formed due to the connection of $[Ag_2(pydc)_2(\mu\text{-en})]^{2-}$ anionic units with dihapto Ag···C interactions [Ag1···C4^{i} = 3.279(6) and Ag1···C5^{i} = 3.318(6) Å, (i) $-x$, 1 − y, 1 − z]. Complex **4** extends to 2D due to the Ag···π interactions of adjacent 1D units [Ag1···Cg1^{ii} = 3.377 Å, Cg1 = N1, C2, C3, C4, C5, C6, (ii) $-x$, $-y$, 1 − z]. The 2D units form strong hydrogen bonds with the cationic $[Cu(en)_2(H_2O)_2]^{2+}$ units that results in a 3D supramolecular structure with 1D pores. When the T5(2) water tapes are removed from the 1D pores, these pores become available for guest H_2 adsorption. The lower H_2 adsorption of complexes **1–3** was attributed to lower pore volume of the materials.

Antimicrobial activity

We performed experiments for microbial activity to understand the potential of complex in biomedical applications. The antimicrobial activity results of the synthesized complexes are presented in Table S10, ESI,† as MIC values (μg mL^{-1}), which is the minimum concentration to inhibit the growth of bacteria or yeast. According to results, the MIC values of the complexes indicate that while the activity of $[Cu(en)_2(H_2O)_2][Ag_2(pydc)_2(\mu\text{-en})]\cdot 6H_2O$ (**4**) was at 47 μg mL^{-1} at all studied microorganisms, the antimicrobial activity of $\{[Cd(H_2O)_4Cu(\mu\text{-pydc})_2]\cdot 2H_2O\}_n$ (**5**) was in the range of 23–187 μg mL^{-1} in the studied microorganisms. The MIC values of $[Cu(\mu\text{-pydc})(dmpen)_2]_n$ (**1**) and $[Cu_2(\mu\text{-pydc})_2(emim)_4]\cdot 2H_2O$ (**2**) were 2250–4500 and 1300 μg mL^{-1}, respectively. As a result, the complexes did not show any difference between the cell wall of bacteria. The complexes did not show any difference in activity according to prokaryote or eukaryote. These complexes have a large effect spectrum on bacteria. The complex $[Cu(en)_2(H_2O)_2][Ag_2(pydc)_2(\mu\text{-en})]\cdot 6H_2O$ (**4**), which contain a Ag molecule, has a higher activity (47 μg mL^{-1} in all studied microorganisms) than the other new complexes.

The antimicrobial activities of some pyridine-2,3-dicarboxylic acid complexes have been reported previously in the literature.[82,83] In recent years, metal complexes are very interesting materials for antimicrobial agents. Biocations such as Co, Ni, Cu, Fe, and metal ions such as Cd, Ag were found to have very high activity in inhibition of bacterial growth.[84] Complex **4** which contains Ag(I) ions has very high activity. It is known from previous studies that many complexes containing Ag(I) are highly effective antimicrobial agents.[84–87] We think that these complexes can be used in treatment of some diseases and disinfection.

Spectroscopic and magnetic properties

Compounds were investigated by FT-IR spectroscopy. Broad bands observed in the range from 3565–3365 cm^{-1} are attributed to the asymmetric and symmetric stretching modes of water molecules in **2**, **4** and **5**. The weak peaks at 2941 and 2685 cm^{-1} are characteristic of aliphatic C–H stretching bands of the CH_3/CH_2/CH groups. This confirms the existence of the dmpen, emim and en ligands in complexes **1–4**. The absence of strong absorption bands around 1720 cm^{-1} indicates the full deprotonation of carboxylate groups of the pydc ligands, as revealed by the X-ray single-crystal structure analysis. The very strong peaks range from 1671–1571 and 1404–1365 cm^{-1} correspond to ν_{asym} and ν_{sym} of the carboxylate group, respectively.

The electronic spectra of water solutions of the complexes **1**, **2**, **4** and **5** display broad absorption bands at 604 (ε = 91 L mol^{-1} cm^{-1}), 646 (ε = 45 L mol^{-1} cm^{-1}), 563 (ε = 62 L mol^{-1} cm^{-1}) and 633 nm (ε = 50 L mol^{-1} cm^{-1}) respectively, which are assigned to the $E_g \rightarrow T_{2g}$ the transition for **1**, **4**, **5** and d_{xz}, $d_{yz} \rightarrow d_{x^2-y^2}$ ($a_1 \rightarrow b_1$) transition for **2**. The strong absorption bands below 300 nm are due to n → π* and π → π* transitions of en, dmpen, emim and pydc ligands.

Photoluminescent properties of **3–5** and $pydcH_2$ were investigated in the crushed single-crystal sample at room temperature. Complexes **3** exhibit intense blue fluorescent emission bands at 406 nm and a shoulder at 483 nm upon excitation at *ca.* 347 nm. These emissions can probably be assigned to the intraligand (π* → π) fluorescent emission because similar emissions are observed at 420 nm and a shoulder at 483 nm for the free pydc. The enhancement of the emissions for **3** may be attributed to the chelation of the ligand to the metal center and ligand enhances conformational rigidity due to their coordination to Cd(II) ions resulting in a decrease in the nonradiative decay of intraligand excited states. Excitation at 335 nm leads to a weak fluorescent emission band with two maxima at about 488 and 537 nm in complex **4**. The first emission peak at 488 nm can probably be assigned to the ligand centered fluorescent emission because similar emissions under the same conditions are observed for the free pydc at 483 nm. Furthermore, the added peak at 537 nm may be attributed to the ligand-to-metal charge transfer (LMCT) bands. The chelation of the ligand to the silver center plays an important role in red shift of the emission. Excitation of the complex **5** at 402 nm produces weak green emission with two maxima at 557 and 598 nm, as shown in Fig. 9. The

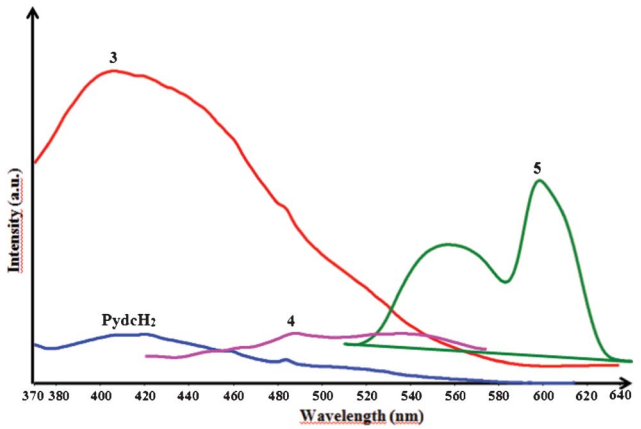

Fig. 9 Photoluminescence emission spectra of **3–5** and $pydcH_2$.

interesting emission of **5** is tentatively assigned as originating from the ligand-to-metal charge-transfer (LMCT) and/or metal-to-ligand charge-transfer (MLCT) character, mixed with metal-centered (ds/dp) states. Ag(I) and Cd(II) complexes usually show photoluminesence emission but Cu(II) ions in hetero-metallic complexes caused a quenching effect. Complex **3** may be a candidate for a light emitting device because of its high thermal stability and the insolubility in many common solvents.

The magnetic properties of complexes in the solid state at room temperature were examined by using a Gouy magnetic balance. The complexes **1**, **2**, **4** and **5** exhibit magnetic moment values of 1.72, 1.73, 1.41 and 1.49 BM, respectively, which correspond to one unpaired electron The measured values for **1** and **2** are quite close to the expected value for copper(II) complexes without interaction. In the case of **4** and **5**, magnetic moments are lower than the expected values for the copper(II) complexes. This may be attributed to the antiferromagnetic coupling interaction between neighbouring Cu(II) ions.

Thermal analyses

Thermal analyses (TG-DTA) were performed to verify the thermal stability of the complexes. The TGA curves showed that **1** and **3** were stable up to 196 and 260 °C, respectively. A total weight loss of 84.20% for **1** and 76.68% for **3** occurred in the temperature range 196–394 and 260–479 °C, respectively, presumably due to the endothermic and exothermic removal of two dmpen for **1** or two emim for **3** and pydc ligands and it is difficult to assign each weight loss separately (for **1**, calcd. 81.6%, DTA_{max} = 204, 227 and 389 °C, $\Delta H = -80.19$ kJ mol^{-1}; for **3**, calcd. 74.21, DTA_{max} = 280 and 468 °C, $\Delta H = -81.01$ kJ mol^{-1}). The thermal decomposition of complex **2** occurs in three stages. The first degradation stage takes place in the range of 57–117 °C and it may correspond to the elimination of two water molecules due to a weight loss of 11.37%, matching well with theoretical value of 11.37% (DTA_{max} = 102 °C). The second stage was attributed to the release of four emim ligands by giving endothermic and exothermic effects, respectively (found 40.29%, calcd. 40.48%, DTA_{max} 227 and 237 °C, $\Delta H = -129.87$ kJ mol^{-1}). The last stage in the temperature range of 256–402 °C may related to the decomposition of two pydc ligands is abruptly burnt by the exothermic effect (found 28.29, calcd. 31.39%, DTA_{max} = 283 °C and 499 °C). For complex **4**, the weight loss starts at *ca.* 45 °C with the liberation of the uncoordinated six water molecules with a weight loss of 13.57% (calcd. 12.03%, $\Delta H = 13.53$ kJ mol^{-1}). In the following endothermic and exothermic stages between 90 and 363 °C, the successive weight-loss stages correspond to the decomposition of en and pydc ligands (DTA_{max} = 141, 261 and 330 °C, found 55.36, calcd. 56.86%, $\Delta H = -89.10$ kJ mol^{-1}). TG and DTA study of **5** shows a weight loss of 18.42% from room temperature to 131 °C, which corresponds to six water molecules (calcd. 17.58%, $\Delta H = 32.31$ kJ mol^{-1}). The anhydrous complex is thermally stable up to about 278 °C. The last stages in the temperature range of 278–427 °C are related to the decomposition of pydc ligands by exothermic effect (found 48.86, calcd. 48.57%, DTA_{max} = 321 and 411 °C, $\Delta H = -115.87$ kJ mol^{-1}). The final products of the thermal decomposition were identified by IR spectroscopy (CuO for **1** and **2**, CdO for **3**, CuO + Ag for **4** and CuO + CdO for **5**).

Conclusion

In summary, we have successfully prepared five new coordination polymers built from 2,3-pyridinedicarboxylic acid. These complexes exhibit structural and dimensional diversity. Complex **1** exhibits a new unexpected coordination mode of pydc. Complex **2** is the first dinuclear complex of copper with pydc, whereas **4** and **5** are also the first 3d–4d heteronuclear complexes. A rare O–H···Ag(I) interaction is seen in **4**. Complex **4** containing 1D water tapes with T5(2) motif has been obtained. Water molecule tapes having T5(2) motif are present within the cavities of the complex and water clusters with hydrogen bonding contribute to the stability of the complex **4**. Complex **5** exhibits rare green emission and the anhydrous form of **5** is thermally stable up to about 278 °C. These results are expected to provide new important information for understanding supramolecular assemblies of pyridine-2,3-dicarboxylate ligand.

Acknowledgements

This work has been supported by The Scientific and Technological Research Council of Turkey (TUBITAK, No. 109T201).

References

1 S. Ma and H. C. Zhou, *Chem. Commun.*, 2010, **46**, 44.
2 L. J. Murray, M. Dinc and J. R. Long, *Chem. Soc. Rev.*, 2009, **38**, 1294.
3 R. J. Kuppler, D. J. Timmons, Q. R. Fang, J. R. Li, T. A. Makal, M. D. Young, D. Yuan, D. Zhao, W. Zhuang and H. C. Zhou, *Coord. Chem. Rev.*, 2009, **253**, 3042.
4 A. U. Czaja, N. Trukhan and U. Müller, *Chem. Soc. Rev.*, 2009, **38**, 1284.

5 S. Takaishi, M. Hosoda, T. Kajiwara, H. Miyasaka, M. Yamashita, Y. Nakanishi, Y. Kitagawa, K. Yamaguchi, A. Kobayashi and H. Kitagawa, *Inorg. Chem.*, 2008, **48**, 9048.
6 S. Kitagawa, R. Kitaura and S. Noro, *Angew. Chem., Int. Ed.*, 2004, **43**, 2334.
7 C. Janiak, *Dalton Trans.*, 2003, 2781.
8 O. Kahn, *Acc. Chem. Res.*, 2000, **33**, 647.
9 S. K. Ghosh, J. Ribas and P. K. Bharadwaj, *Cryst. Growth Des.*, 2005, **5**, 623.
10 B. B. Ding, Y. Q. Weng, Z. W. Mao, C. K. Lam, X. M. Chen and B. H. Ye, *Inorg. Chem.*, 2005, **44**, 8836.
11 G. R. Desiraju, *Acc. Chem. Res.*, 2002, **35**, 565.
12 G. Guilera and J. W. Steed, *Chem. Commun.*, 1999, 1563.
13 C. A. Hunter, K. R. Lawson, J. Perkins and C. J. Urch, *J. Chem. Soc., Perkin Trans. 2*, 2001, 651.
14 C. Janiak, *J. Chem. Soc., Dalton Trans.*, 2000, 3885.
15 D. Braga, F. Grepioni and E. Tedesco, *Organometallics*, 1998, **17**, 2669.
16 A. Sediki, F. Lebsir, L. Martiny, M. Dauchez and A. Krallafa, *Food Chem.*, 2008, **106**, 1476.
17 Y. Jin, Y. Che, S. Batten, P. Chen and J. Zheng, *Eur. J. Inorg. Chem.*, 2007, 1925.
18 M. Mascal, L. Infantes and J. Chisholm, *Angew. Chem., Int. Ed.*, 2005, **45**, 32.
19 R. Ludwig, *Angew. Chem., Int. Ed.*, 2001, **40**, 1808.
20 S. Noro, S. Kitagawa, M. Yamashita and T. Wada, *Chem. Commun.*, 2002, 222.
21 S. Kitagawa, S. Noro and T. Nakamura, *Chem. Commun.*, 2006, 701.
22 B. Hoskins and R. Robson, *J. Am. Chem. Soc.*, 1990, **112**, 1546.
23 S. M. Humphrey, T. J. P. Angliss, M. Aransay, D. Cave, L. A. Gerrard, G. F. Weldon and P. T. Wood, *Z. Anorg. Allg. Chem.*, 2007, **633**, 2342.
24 L. Carlucci, G. Ciani, S. Maggini, D. M. Proserpio and M. Visconti, *Chem.–Eur. J.*, 2010, **16**, 12328.
25 G. H. Wang, Z. G. Li, H. Q. Jia, N. H. Hu and J. W. Xu, *Acta Crystallogr., Sect. E: Struct. Rep. Online*, 2009, **65**, 1568.
26 M. Andruh, J. P. Costes, C. Diaz and S. Gao, *Inorg.Chem.*, 2009, **48**, 3342.
27 A. Lazarescu, S. Shova, J. Bartolome, P. Alonso, A. Arauzo, A. M. Balu, Y. A. Simonov, M. Gdaniec, C. Turta, G. Filoti and R. Luque, *Dalton Trans.*, 2011, **40**, 463.
28 M. Li, J. Xiang, L. Yuan, S. Wu, S. Chen and J. Sun, *Cryst. Growth Des.*, 2006, **6**, 2036.
29 Z. Yu, G. Li, Y. Jiang, J. Xu and J. Chen, *Dalton Trans.*, 2003, 4219.
30 H. Yin and S. X. Liu, *J. Mol. Struct.*, 2009, **918**, 165.
31 T. K. Maji, G. Mostafa, R. Matsuda and S. Kitagawa, *J. Am. Ceram. Soc.*, 2005, **127**, 17152.
32 B. O. Patrick, C. L. Stevens, A. Storr and R. C. Thompson, *Polyhedron*, 2003, **22**, 3025.
33 Y. Kang, H. Zhang, Z. J. Li, H. K. Cheng and Y. G. Yao, *Inorg. Chim. Acta*, 2006, **359**, 2201.
34 S. Natarajan, S. Manual, P. Mahata, V. Rao, P. Ramaswamy, A. Banerjee, A. Paul and K. Ramya, *J. Chem. Sci.*, 2006, **118**, 525.
35 M. Goher, A. Youssef and F. Mautner, *Polyhedron*, 2006, **25**, 1531.
36 M. Frisch and C. L. Cahill, *Dalton Trans.*, 2006, 4679.
37 Y. Zhou, X. Shen, C. Du, B. Wu and H. Zhang, *Eur. J. Inorg. Chem.*, 2008, 4280.
38 E. J. Gao, M. C. Zhu, Y. Huang, L. Liu, H. Y. Liu, F. C. Liu, S. Ma and C. Y. Shi, *Eur. J. Med. Chem.*, 2010, **45**, 1034.
39 Q. Yue, J. Yang, G. Li, G. Li, W. Xu, J. Chen and S. Wang, *Inorg. Chem.*, 2005, **44**, 5241.
40 W. Starosta and J. Leciejewicz, *J. Coord. Chem.*, 2009, **62**, 1240.
41 M. P. Heyes, B. J. Brew, A. Martin, R. W. Price, A. M. Salazar, J. J. Sidtis, J. A. Yergey, M. M. Mouradian, A. E. Sadler and J. Keilp, *Ann. Neurol.*, 1991, **29**, 202.
42 A. Schurr, C. A. West and B. M. Rigor, *Brain Res.*, 1991, **568**, 199.
43 A. Vezzani, R. Serafini, M. Stasi, S. Caccia, I. Conti, R. Tridico and R. Samanin, *J. Pharmacol. Exp. Ther.*, 1989, **249**, 278.
44 A. C. Foster, A. Vezzani, E. D. French and R. Schwarcz, *Neurosci. Lett.*, 1984, **48**, 273.
45 R. Schwarcz, W. O. Whetsell and R. M. Mangano, *Science*, 1983, **219**, 316.
46 B. Zhao, X. Y. Chen, P. Cheng, D. Z. Liao, S. P. Yan and Z. H. Jiang, *J. Am. Chem. Soc.*, 2004, **126**, 15394.
47 M. D. Allendorf, C. A. Bauer, R. K. Bhakta and R. J. T. Houk, *Chem. Soc. Rev.*, 2009, **38**, 1330.
48 B. Chen, L. Wang, F. Zapata, G. Qian and E. B. Lobkovsky, *J. Am. Chem. Soc.*, 2008, **130**, 6718.
49 B. Chen, Y. Yang, F. Zapata, G. Lin, G. Qian and E. B. Lobkovsky, *Adv. Mater.*, 2007, **19**, 1693.
50 B. D. Chandler, D. T. Cramb and G. K. H. Shimizu, *J. Am. Chem. Soc.*, 2006, **128**, 10403.
51 E. Y. Lee, S. Y. Jang and M. P. Suh, *J. Am. Chem. Soc.*, 2005, **127**, 6374.
52 W. J. Rieter, K. M. L. Taylor, H. An and W. Lin, *J. Am. Chem. Soc.*, 2006, **128**, 9024.
53 E. C. Yang, Q. Q. Liang, P. Wang and X. J. Zhao, *Inorg. Chem. Commun.*, 2009, **12**, 211.
54 C. S. Liu, Z. Chang, J. J. Wang, L. F. Yan, X. H. Bu and S. R. Batten, *Inorg. Chem. Commun.*, 2008, **11**, 889.
55 J. He, J. X. Zhang, G. P. Tan, Y. G. Yin, D. Zhang and M. H. Hu, *Cryst. Growth Des.*, 2007, **7**, 1508.
56 K. L. Zhang, F. Zhou, L. M. Yuan, G. W. Diao and S. W. Ng, *Inorg. Chim. Acta*, 2009, **362**, 2510.
57 L. Wang, L. Duan, E. Wang, D. Xiao, Y. Li, Y. Lan, L. Xu and C. Hu, *Transition Met. Chem.*, 2004, **29**, 212.
58 P. Kanoo, R. Matsuda, R. Kitaura, S. Kitagawa and T. K. Maji, *Inorg. Chem.*, 2012, **51**, 9141.
59 (*a*) G. M. Sheldrick, *SHELXS-97, Program for solution of crystal structures*, University of Göttingen, Germany, 1997; (*b*) G. M. Sheldrick, *SHELXL-97, Program for refinement of crystal structures*, University of Göttingen, Germany, 1997.
60 C. F. Macrae, P. R. Edgington, P. McCabe, E. Pidcock, G. P. Shields, R. Taylor, M. Towler and J. van De Streek, *J. Appl. Crystallogr.*, 2006, **39**, 453.
61 D. Frenkel and B. Smit, *Understanding Molecular Simulation: From Algorithms to Applications*, Academic Press, San Diego, 2nd edn, 2002.
62 S. Keskin, J. Liu, R. B. Rankin, J. K. Johnson and D. S. Sholl, *Ind. Eng. Chem. Res.*, 2009, **48**, 2355.
63 A. K. Rappe, C. J. Casewit, K. S. Colwell, W. A. Goddard and W. M. Skiff, *J. Am. Chem. Soc.*, 1992, **114**, 10024.
64 V. Buch, *J. Chem. Phys.*, 1994, **100**, 7610.

65 S. Y. Jiang, K. E. Gubbins and J. A. Zollweg, *Mol. Phys.*, 1993, **80**, 103.
66 A. I. Skoulidas and D. S. Sholl, *J. Phys. Chem. A*, 2003, **107**, 10132.
67 D. Frenkel and B. Smit, *Understanding Molecular Simulation: From Algorithms to Applications*, Academic Press, London, 1996.
68 O. Z. Yesilel, G. Günay, A. Mutlu, H. Ölmez and O. Büyükgüngör, *Inorg. Chem. Commun.*, 2010, **13**, 1173.
69 O. Z. Yesilel, H. Erer and O. Büyükgüngör, *Inorg. Chem. Commun.*, 2009, **12**, 724.
70 Y. Y. Lin, G. H. Chen, Y. P. Yu and B. X. Liu, *Acta Crystallogr., Sect. E: Struct. Rep. Online*, 2007, **63**, m2178.
71 H. Aghabozorg, R. Khadivi, M. Ghadermazi, H. Pasdar and S. Hooshmand, *Acta Crystallogr., Sect. E: Struct. Rep. Online*, 2008, **64**, m267.
72 S. Martinez-Vargas, R. A. Toscano and J. Valdes-Martinez, *Acta Crystallogr., Sect. E: Struct. Rep. Online*, 2007, **63**, m1975.
73 S. Shit, J. Chakraborty, S. Sen, G. Pilet, C. Desplanches and S. Mitra, *J. Mol. Struct.*, 2008, **891**, 19.
74 T. Suga and N. Okabe, *Acta Crystallogr., Sect. C: Cryst. Struct. Commun.*, 1996, **52**, 1410.
75 D. R. Turner and S. R. Batten, *Acta Crystallogr., Sect. E: Struct. Rep. Online*, 2007, **63**, m452.
76 D. M. Roe, P. M. Bailey, K. Moseley and P. M. Maitlis, *J. Chem. Soc., Chem. Commun.*, 1972, 1237.
77 M. Brookhart, M. L. H. Green and G. Parkin, *Proc. Natl. Acad. Sci. U. S. A.*, 2007, **104**, 6908.
78 L. Infantes and S. Motherwell, *CrystEngComm*, 2002, **4**, 454.
79 D. Braga, F. Grepioni, E. Tedesco, K. Biradha and G. R. Desiraju, *Organometallics*, 1997, **16**, 1846.
80 A. L. Myers and J. M. Prausnitz, *AIChE J.*, 1965, **11**, 121.
81 R. Krishna and D. Paschek, *Phys. Chem. Chem. Phys.*, 2001, **3**, 453.
82 A. T. Colak, Y. Sahin, O. Z. Yesilel, F. Colak, F. Yilmaz and M. Tas, *Inorg. Chim. Acta*, 2012, **383**, 169.
83 P. Sengupta, S. Ghosh and T. C. W. Mak, *Polyhedron*, 2001, **20**, 975.
84 O. Z. Yesilel, G. Gunay, C. Darcan, M. S. Soylu, S. Keskin and S. W. Ng, *CrystEngComm*, 2012, **14**, 2817.
85 O. Z. Yesilel, A. Mutlu, C. Darcan and O. Buyukgungor, *J. Mol. Struct.*, 2010, **964**, 39.
86 M. Rai, A. Yadav and A. Gade, *Biotechnol. Adv.*, 2009, **27**, 76.
87 A. Jurjus, B. S. Atiyeh, I. M. Abdallah, R. A. Jurjus, S. N. Hayek, M. A. Jaoude, A. Gerges and R. A. Tohme, *Burns*, 2007, **33**, 892.

